J. MATER. CHEM., 1995, 5(11), 1919–1925

Preparation, Physical and Structural Characterization of $LiMnO_2$ Samples with Variable Cationic Disorder

Laurence Croguennec,*[a] Philippe Deniard,[a] Raymond Brec[a] and André Lecerf[b]
[a] *Laboratoire de Chimie des Solides, I.M.N. (C.N.R.S.), 2 rue de la Houssinière, 44072, Nantes cedex 03, France*
[b] *Laboratoire de Chimie des Solides, I.N.S.A. de Rennes, 20 avenue des Buttes de Couesmes, 35073 Rennes cedex, France*

Orthorhombic $LiMnO_2$ samples, synthesized at high temperatures from a mixture of $LiOH{\cdot}H_2O$ and Mn_2O_3 under a reducing atmosphere, have been fully characterized. The morphology showed that important differences exist between two sets of materials: A-type materials prepared with a deficiency of LiOH with respect to the $LiMnO_2$ stoichiometric composition and B-type materials prepared with an excess of LiOH. Bulk density variations were interpreted in terms of the occurrence of several lithium and/or manganese salt impurities. From Rietveld refinements, and contrary to the previously described $LiMnO_2$ structures, the present $LiMnO_2$ samples exhibit a cationic disorder on the lithium and manganese sites, with occupancy variations ranging from 3 to 12%. Finally, the frequently occurring abnormal widening of the second diffraction line could be modelled and attributed to the mixing of a regular diffraction peak of the phase under study [the (110) reflection] and of some poorly crystallized unreacted Mn_2O_3. These structural results can be used to explain the electrochemical behaviour of the samples when employed as cathodes in rechargeable lithium batteries.

Over the last 20 years, the $LiMnO_2$ phases have been the subject of many studies because, like $LiNiO_2$ and $LiCoO_2$, they are very active cathodic materials, often used in rechargeable electrochemical lithium batteries. The intense research on the manganese phases has also been motivated because manganese is non-toxic and its oxides are cheap. In addition, Mn presents the advantage of exhibiting the oxidation state IV in MnO_2, allowing for good stabilization of the oxidized $LiMnO_2$.

The search for electrochemically highly reactive phases led many groups to imagine new soft chemistry ways to prepare manganese dioxides (with or without lithium). So, a new low-temperature ($300 < T/°C < 450$) synthesis of orthorhombic $LiMnO_2$ was implemented by Ohzuku *et al.*[1] It consisted of heating a pressed pellet of an equimolecular mixture of manganite (γ-MnOOH) and lithium hydroxide ($LiOH{\cdot}H_2O$) under nitrogen for 15 h. More recently, Reimers *et al.*[2] proposed an improvement of the Ohzuku method. They showed that $LiMnO_2$ could be readily prepared at very low temperature (100 °C) through an ion-exchange reaction.

The compounds synthesized at higher temperatures ($T/°C > 450$ °C) generally present electrochemical capacities smaller than the phases obtained at low temperature. The improved electrochemical properties of the low-temperature phases have been tentatively attributed to disorder (*i.e.* to stacking faults), a characteristic which would be responsible for the poor crystallization state of the phases [wide diffraction peaks in the X-ray diffraction (XRD) diagrams]. A higher-temperature synthesis ($600 < T/°C < 620$) has been used by Gummow *et al.*[3] to prepare an orthorhombic $LiMnO_2$. The phase was prepared under argon from a mixture of γ-MnO_2 and LiOH, with carbon as a reducing agent. Poor electrochemical reactivity led to a capacity of only 70 mA h g^{-1} when the phase was put into use in a lithium battery. This result reinforced the idea that high-temperature-prepared $LiMnO_2$ materials were not appropriate as cathodic materials for use in lithium rechargeable batteries. However, recently Davidson *et al.*[4] prepared the same orthorhombic lithium–manganese dioxide at high temperature, and, unexpectedly, the phase showed rather elevated specific capacities of about 140 mA h g^{-1}. The synthesis consists of firing a mixture of β-MnO_2 and Li_2CO_3 between 600 and 650 °C in a first step to eliminate CO_2, followed by heating the sample between 800 and 1000 °C under an argon flux. The improved performances have been observed, but not explained.

We recently prepared a new high-temperature orthorhombic $LiMnO_2$ according to a newly patented procedure.[5] Preliminary results have shown that this compound which is used as a cathode in $LiMnO_2$/Li electrochemical systems, presents a mean discharge potential of around 3.5 V, with the best batteries reaching a capacity higher than 160 mA h g^{-1} with rather good cyclability.[5] Because the phase atomic structure characteristics are believed to be the key to the unexpectedly high electrochemical energy of this new high-temperature-formed manganese oxide, a complete and thorough structural and physical study of $LiMnO_2$ has been undertaken. This article reports the full characterization of this phase.

$LiMnO_2$ Synthesis

The synthesis of the orthorhombic $LiMnO_2$ phase has been performed by mixing Mn_2O_3 (prepared by thermolysis of MnO_2 under air at 700 °C) and $LiOH{\cdot}H_2O$ (commercial product used as received) in 1/*ca.* 2 proportions. The synthesis consists of successive grindings and heatings at 300, 500 and 700 °C. The final temperature of 700 °C is maintained for 4 h before allowing the sample to cool slowly to room temperature. The preparation cannot be made under air, because the phase reacts with oxygen to give a mixture of Li_2MnO_3 and $LiMn_2O_4$. The synthesis was hence performed under an inert gas (argon for instance) or under a mildly reducing atmosphere (nitrogen mixed with hydrogen). The nominal Li/Mn chosen ratios ranged from 0.95 to 1.10 in order to try to obtain various non-stoichiometries around the $LiMnO_2$ compositions. This corresponded to two series of samples with $Li/Mn \leqslant 1$ (labelled A) and $Li/Mn > 1$ (labelled B) totalling six samples in all. The Mn and Li elemental analyses performed on the samples revealed ratios slightly different from the nominal values (Table 1). In addition, redox analyses demonstrated the absence of Mn^{IV} and Mn^{II} species, pointing to a $LiMnO_2$ stoichiometry in the preparations. Accordingly,

Table 1 Analytical Li/Mn ratio [$(Li/Mn)_{obs}$], density and overall characteristics of the XRD diagrams *vs.* targetted compositions [$(Li/Mn)_{nominal}$] for the $LiMnO_2$ samples; [the thickness of the (110) diffraction line and the resolution of the (310)/(230) doublet indicate a better definition of the diagram and larger crystal size in agreement with SEM observations]

	A-type samples			B-type samples		
	MN389	MN384	MN386	MN399	MN412	MN401
$(Li/Mn)_{nominal}$	0.95	0.98	1.00	1.06	1.08	1.10
$(Li/Mn)_{obs}$	0.96	0.98	1.00	1.03	1.05	1.06
density	4.246(5)	4.224(1)	4.223(3)	4.179(1)	4.157(3)	4.038(1)
(110) line	wide	wide	thin	thin	thin	thin
(310)/(230) peak	not resolved	not resolved	not resolved	resolved	resolved	resolved

the various samples will be labelled $LiMnO_2$ throughout the paper.

Hoppe *et al.*[6] prepared an orthorhombic modification of $LiMnO_2$, a material reported to be stoichiometric, with a brown–black colour. The materials prepared according to the above method[5] are light-green or black. The light-green colour corresponds to A-type materials and the black colour to the B-type ones. Colour is therefore the first visible criterion that allows the differentiation between the Hoppe phases and some of those of the present study. The differences may originate either in the composition of the phases (departure from $LiMnO_2$ stoichiometry) or in a grain size effect, well known, for instance, in pigments.

The presence of some impurities (Li_2CO_3, Li_2SO_4 and MnO) was clearly demonstrated in the $LiMnO_2$ samples prepared according to ref. 5. MnO was detected by XRD in the materials referenced MN389 and MN384 [revealed through a small peak at the foot of the (011) line ($2\theta = 35°$) and another one at $2\theta = 59°$]. The occurrence of lithium sulfate and carbonate was demonstrated by IR spectroscopy and elemental analysis. The IR spectra show vibrations characteristic of lithium sulfate at 1150 and 1000 cm^{-1} and of lithium carbonate at 1490, 1430 and 860 cm^{-1} (Fig. 1). The analysis of C, S, Li and Mn yielded a maximum content of about 0.2 and 4 wt.% for the sulfate and the carbonate, respectively. There was no hydrogen, as also confirmed by the absence of incoherent scattering in the powder neutron diffraction diagrams, which were recorded at the Laboratoire Léon Brillouin (Laboratoire commun CEA-CNRS, Saclay, France). The presence of lithium carbonate (resulting in the carbonation of LiOH) was also confirmed by the neutron diffraction study and by differential scanning calorimetry (Fig. 2) showing, in the latter case, a phase transition at 723 °C corresponding well to Li_2CO_3 fusion.

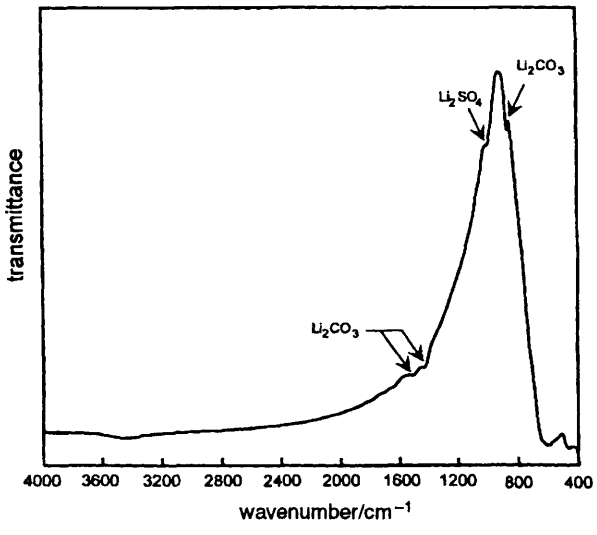

Fig. 1 IR spectrum of sample MN412. Arrows indicate the vibrations attributed to two impurities often found in the $LiMnO_2$ samples. For this particular example, the maximum weight concentrations of Li_2SO_4 and Li_2CO_3 are *ca.* 0.2 and 4%.

Physical Characterization

Morphology

A scanning electron microscopy (SEM) study performed with a JEOL 6400F instrument allowed comparison of the A- and B-type materials. The former group presents a homogeneous size distribution of regular, elongated grains, parallelepipedic in shape (Fig. 3). The grain sizes span from *ca.* 0.2 to 1 μm. The latter group shows (Fig. 4) a large grain size distribution with very ill-defined shapes. Whereas the large grains are embedded within one another, the smaller grains are scattered around the larger ones (diameter of large grains, *ca.* 10 μm, and of small grains, *ca.* 1 μm). Thus the larger grains of the B-type samples are about ten times the size of those of the A-type samples. Note that the green samples correspond, as expected, to the smaller grains.

Density

Density measurements have been made with an automated ACCUPYC 1330 pycnometer. The data show that the A-type samples have very similar densities [identical within three estimated standard deviations (ESD)]. The densities of the B-type materials, notably lower than those of the other group, decrease with the observed Li/Mn bulk ratio (Table 1).

Description of the $LiMnO_2$ Model Structure

The stoichiometric, orthorhombic $LiMnO_2$ compound presents a *Pmnm* space group, with $Z = 2$, Mn and Li being in the 2a special position (on a symmetry element) with an octahedral coordination of oxygen atoms (in the 2b special

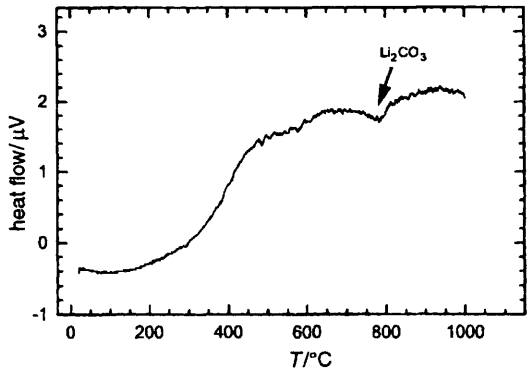

Fig. 2 Differential thermal analysis of sample MN412 showing the fusion of Li_2CO_3 at 723 °C

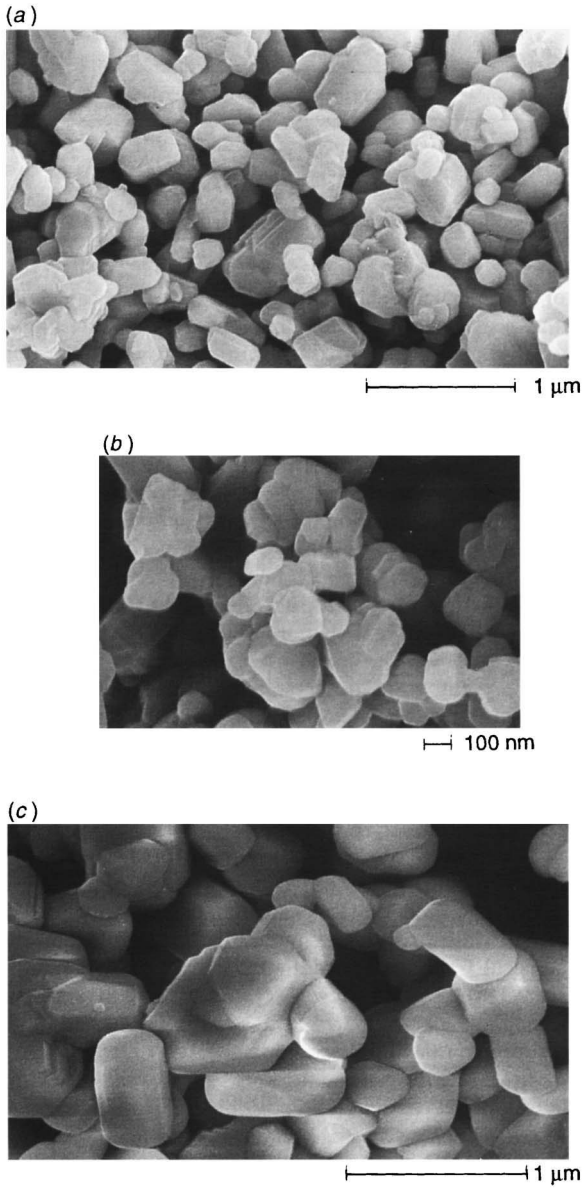

Fig. 3 Morphology of the A-type samples. A homogeneous grain size distribution is observed (grain size *ca.* 0.2–1 μm). (*a*) MN389, (*b*) MN384, (*c*) MN386.

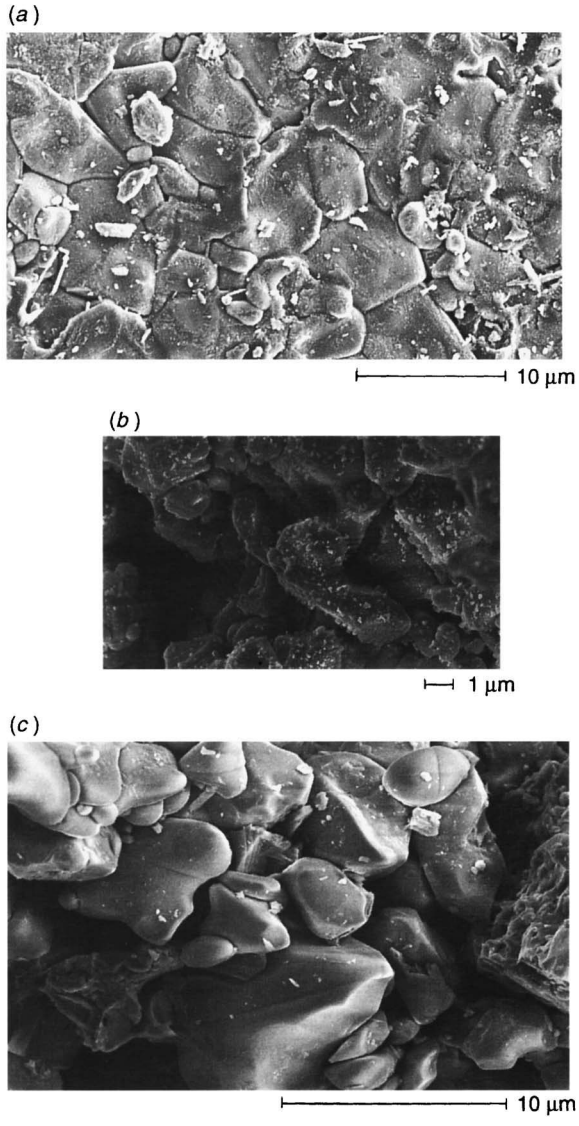

Fig. 4 Morphology of the B-type samples. A large grain size distribution can be observed (grain size *ca.* 10–1 μm). (*a*) MN399, (*b*) MN412, (*c*) MN401.

positions).[1–4,6] Fig. 5 shows a projection of the structure along the ***c*** axis. The structure is built up from MnO_6 octahedra sharing apices along the ***a*** axis and edges along the ***c*** axis, so that the structure exhibits a succession of corrugated $(MnO_6)_n$ and $(LiO_6)_n$ slabs. As previously reported by Reimers *et al.*[2] it can be described as a cation superlattice structure of a rock salt structure of MnO.

Considering that lithium and manganese are similar sized ions ($r_{i(Mn^{III})}=0.645$ Å and $r_{i(Li^{I})}=0.76$ Å)[7] and that they play a perfectly symmetrical role in the structure, a lithium/manganese substitution can be envisaged within the hypothesis of cationic disorder. Within the same slab, there could be LiO_6 and MnO_6 octahedra simultaneously present. Such a hypothesis has not been considered in the $LiMnO_2$ structures published to date.[1–4,6]

X-Ray Diffraction Study of the $LiMnO_2$ Phases

Characterization of the Powders

The X-ray powder diffraction diagrams of the different $LiMnO_2$ samples were obtained on a SIEMENS D5000

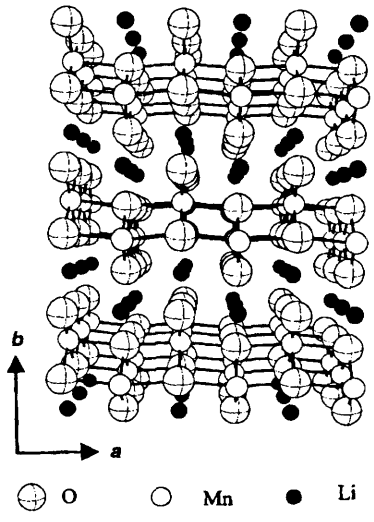

Fig. 5 Projection of $LiMnO_2$ along the ***c*** axis. The two-dimensional arrangement is made up of corrugated slabs of MnO_6 and LiO_6 octahedra sharing edges and corners.

Table 2 Full pattern matching $LiMnO_2$ refined parameters: the cell parameters values can be compared with those obtained by Hoppe *et al.*[6]

	A-type samples			B-type samples			
	MN389	MN384	MN386	MN399	MN412	MN401	Hoppe
a/Å	4.5777(2)	4.5807(2)	4.5824(2)	4.5758(9)	4.5753(1)	4.5770(9)	4.572
b/Å	5.7480(3)	5.7487(4)	5.7524(3)	5.7516(2)	5.7504(2)	5.7559(1)	5.757
c/Å	2.8052(1)	2.8048(2)	2.8067(1)	2.8062(1)	2.8061(1)	2.8076(1)	2.805
V/Å^3	73.83(1)	73.86(1)	73.99(1)	73.85(2)	73.84(1)	73.97(2)	73.8

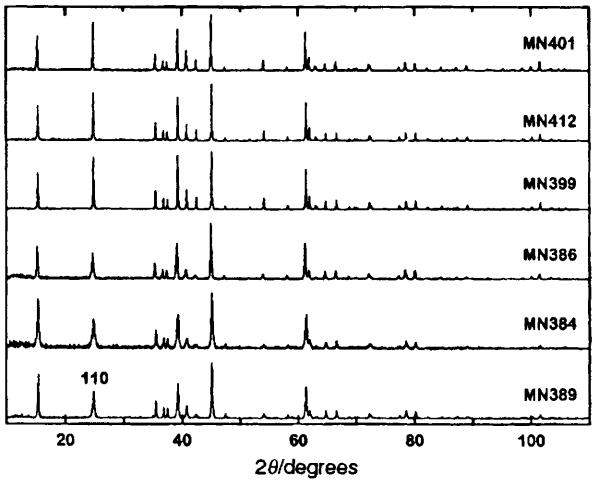

Fig. 6 General features of the X-ray powder diffraction diagrams of the $LiMnO_2$ samples. Note the large width of the $2\theta \approx 28°$ peak [(110) line] of some samples.

diffractometer in reflection geometry, without a monochromator (Cu-$K_{\alpha 1}$ = 1.540598 Å, Cu-$K_{\alpha 2}$ = 1.544390 Å). The parameters refined with a full pattern matching program[8] are given in Table 2 and the XRD diagrams are shown in Fig. 6.

The (110) reflection ($2\theta = 24.8°$) is sometimes very wide compared with the other peaks of the diagram (Table 1) and its intensity varies regularly from sample to sample on going from MN389 to MN401. In addition, around $2\theta = 63°$, a peak, with (310)/(230) indexing, appears either as a singlet or a doublet. In some phases, the doublet is perfectly separated, but in others not at all (Table 1), depending on the crystallite sizes. Clearly, the (110) and (310)/(230) diffraction lineshapes give qualitative indications of the state of crystallinity of the phase. Indeed, as observed by SEM (Fig. 4), larger grains (B-type samples) give a thinner (110) line and a better separation of the (310)/(230) doublet.

Grain Size Anisotropy

Because of the non-monotonic variation of the reflection linewidths with 2θ for the $LiMnO_2$ samples [a problem linked, in particular, to the (110) line at $2\theta = 24.8°$], the grain size anisotropy was studied by the Warren–Averbach method.[9] This method has been put in use with the WIN-CRYSIZE software,[10] to allow crystallite size and microstrain determinations. The experimental data necessary for the calculations are the peaks widths at half maximum (FWHM) and the Gaussian–Lorentzian η mixing factors for the sample reflections and those of LaB_6 used as standard. These data were obtained from the PROFILE program.[11] Table 3 presents the results obtained. The samples MN384 and MN389 are characterized by grain size anisotropy (longer along ***b***), corresponding to the small and well shaped crystals observed by SEM and to the wider diffraction lines (non-separated peak at $2\theta = 63°$). In addition, the growth axes of the needle-like crystals (Fig. 3) do correspond to ***b***. For the other materials, the anisotropy is less obvious in agreement with the larger, not so well shaped crystals, with more well resolved XRD patterns. This is in accord with the fact that the samples MN399 and MN401 present grain or crystallite sizes about one order larger than those of MN389, MN384 and MN386.

Structure Refinement of the $LiMnO_2$ Samples from the Hoppe Model

When it proved necessary, *i.e.* for the MN389 and MN384 samples, the (110) reflection ($2\theta \approx 24.8°$) was removed from the powder diffraction Rietveld refinement. In effect, the abnormal width of this very intense reflection did not allow for classical Cagliotti linewidth refinement as a function of 2θ [$(\mathrm{FWHM})^2 = utg^2\theta + vtg\theta + w$]. As discussed later, this abnormal line is not due to $LiMnO_2$ only. This point allowed us to suppress this ill-defined line.

In a first step, the XRD data were refined using the Hoppe structural model[6] with atomic position 2a for manganese and lithium, and 2b for oxygen. Because the atomic displacement parameters (ADP) were difficult to refine (even Hoppe refinement from single-crystal data led to non-homogeneous ADPs, see Table 4 caption), the isotropic ADPs of the refinements were fixed at 0.5 Å^2 for Mn and 1.00 Å^2 for Li and for O. (For Mn, the value corresponds to that generally found for this element in single-crystal studies and that for lithium corresponds to the lower value obtained in other similar studies.[12–16]) In the case of oxygen, the calculated B_{iso} values vary wildly from 0.5 to >4.0 Å^2; an intermediate value has been chosen, such that a small variation around it (± 0.5 Å^2) induced little change in the structural results. Table 4 summarizes the values of the cell parameters and of the atomic positions obtained with this model. Note that the cell volumes are very similar, suggesting that the compounds all present $LiMnO_2$ stoichiometry.

As the results show, these values are not significantly

Table 3 Crystallite size determination obtained with the Warren–Averbach method in the ***a***, ***b*** and ***c*** directions of the $LiMnO_2$ cells (for MN412 the crystallite size cannot be determined by the Warren–Averbach method because it is too highly crystalline)

	A-type samples			B-type samples		
	MN389	MN384	MN386	MN399	MN412	MN401
D_{h00}/Å	350	420	350	1930	—	885
D_{0k0}/Å	860	850	475	1685	—	870
D_{00l}/Å	560	430	505	2015	—	760

Table 4 Cell parameters and atomic positions of the Rietveld-refined $LiMnO_2$ samples with an ordered model based on Hoppe[6] results[a]

	A-type samples			B-type samples			
	MN389	MN384	MN386	MN399	MN412	MN401	Hoppe
a/Å	4.5780(2)	4.5810(2)	4.5826(3)	4.5758(1)	4.5751(1)	4.5771(1)	4.572
b/Å	5.7486(4)	5.7487(5)	5.7523(4)	5.7516(2)	5.7506(1)	5.7561(2)	5.757
c/Å	2.8053(1)	2.8046(2)	2.8068(2)	2.8062(1)	2.8061(1)	2.8076(1)	2.805
V/Å^3	73.82(1)	73.86(1)	73.99(1)	73.85(2)	73.829(6)	73.97(2)	73.8
y (Mn)	0.6317(7)	0.6385(7)	0.6352(8)	0.6363(5)	0.6361(5)	0.6352(6)	0.6347(2)
y (Li)	0.092(8)	0.103(5)	0.121(8)	0.097(5)	0.099(5)	0.097(5)	0.926(4)
y [O(1)]	0.132(3)	0.139(4)	0.138(3)	0.126(2)	0.131(2)	0.128(3)	0.144(1)
y [O(2)]	0.617(3)	0.608(3)	0.610(3)	0.604(2)	0.603(2)	0.601(2)	0.602(1)
χ^2	5.71	1.98	3.95	4.42	2.72	4.01	—
R_{wp}	6.19	4.14	4.15	4.72	3.65	4.26	6.68

[a] The isotropic ADPs were fixed at 0.5 Å^2 for Mn and 1.0 Å^2 for Li and O. (Those of the Hoppe single-crystal refinement were $B_{iso\,(Mn)}$ = 0.27 Å^2, $B_{iso\,(Li)}$ = 1.8 Å^2, $B_{iso\,[O(1)]}$ = 0.3 Å^2 and $B_{iso\,[O(2)]}$ = 1.1 Å^2.)

different from those obtained by Hoppe.[6] Despite the very good reliability factors, this structural model was not found to be the most appropriate for the $LiMnO_2$ materials synthesized according to the method of ref. 5. In effect, certain diffraction regions still remained poorly modelled. Since the lithium and manganese ions have a similar size and fill the same type of octahedral site, Li/Mn substitution was attempted. In such a hypothesis, a single slab will then contain MnO_6 and LiO_6 groups and the model will thus correspond to cationic disorder.

Structure Refinement with Cationic Disorder

Within the frame of cationic disorder, the occupation ratios of lithium and manganese on each site have been refined and normalised with respect to the other cation. Similarly, the substitution rates of Li and Mn on the Mn and Li sites, respectively, have been constrained to be equal. On the same site, the Mn and Li atoms were indeed constrained to have the same atomic positions, with the ADPs fixed at the above values. Table 5 lists the cell parameters, atomic positions and occupation ratios using the disordered model.

The reliability factors (Table 5) and fitting of the XRD patterns (see Fig. 7 for MN412 as an example) are clearly better with the introduction of Li/Mn substitution. However, it was necessary to check the validity of the procedure, since the improved results could be due simply to the increase in the number of refined parameters. Using the deviance test[8] (analogous to the Hamilton test used in single-crystal structure determinations) it is possible to determine whether the lowering of χ^2 (the goodness-of-fit factor used to evaluate the quality of the Rietveld refinement) is to be attributed to an increase in the number of variables or to the amelioration of the structural model. The deviance, D, is defined as follows:

$$D = 2\sum_{i=1}^{N}\left\{y_i \ln\frac{y_i}{y_{ci}} - (y_i - y_{ci})\right\}$$

where y_i and y_{ci} are the observed and calculated intensities and N is the number of recorded data points. The deviance thus takes into account the quality of the refinement model and the number of parameters used. The deviance criterion,

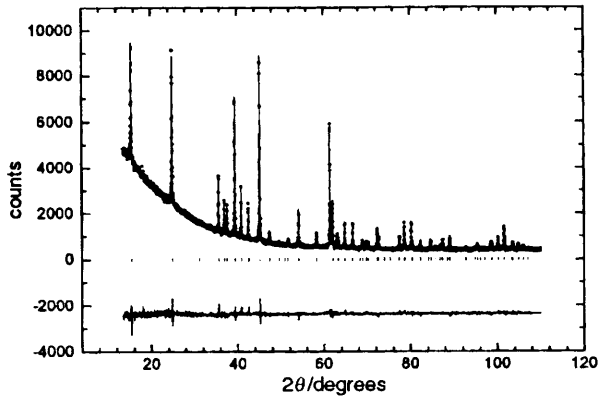

Fig. 7 X-Ray powder diffraction Rietveld refinement diagram of sample MN412 taking into account the disorder between lithium and manganese. A satisfactory refinement is achieved for this compound, as well as with all the other $LiMnO_2$ phases (see Table 5).

Table 5 Cell parameters and atomic positions of the Rietveld-refined $LiMnO_2$ samples with a disordered model (a sizeable improvement of the fit is observed with a measurable and significant site substitution)

	A-type samples			B-type samples		
	MN389	MN384	MN386	MN399	MN412	MN401
a/Å	4.5780(2)	4.5809(2)	4.5825(2)	4.5758(1)	4.5752(1)	4.5771(1)
b/Å	5.7488(3)	5.7487(4)	5.7526(3)	5.7517(1)	5.7506(1)	5.7561(2)
c/Å	2.8054(1)	2.8047(2)	2.8067(1)	2.8062(1)	2.8061(1)	2.8076(1)
V/Å^3	73.83(1)	73.86(1)	73.99(1)	73.86(2)	73.829(6)	73.97(2)
y (Mn)	0.630(1)	0.633(1)	0.6303(8)	0.6322(4)	0.6339(5)	0.6323(5)
y (Li)	0.099(5)	0.095(5)	0.093(3)	0.071(2)	0.084(3)	0.078(3)
y [O(1)]	0.132(6)	0.134(4)	0.139(3)	0.116(1)	0.126(2)	0.121(2)
y [O(2)]	0.612(5)	0.605(3)	0.607(3)	0.593(1)	0.597(2)	0.593(2)
Li/Mn substitution rate (%)	7.1(3)	6.5(3)	9.9(2)	6.0(2)	3.3(2)	4.2(2)
R_{wp}	5.50	3.67	3.35	4.26	3.50	4.08
χ'^2	4.50	1.55	2.57	3.59	2.51	3.70
$(1-\chi'^2/\chi^2)$ (%)	21	22	35	19	8	8

Q, is defined as:

$$Q = D + \alpha P_{max}$$

where P_{max} is the number of refined parameters and $\alpha = 2$ or $\ln P_{max}$.[8]

The model presenting the lowest Q value is considered the better to describe the structure. The results obtained for the six studied materials (Table 6) show that, with a substantially lower Q value, we are justified in choosing the Li/Mn substitution model to describe the structure of the phases under study. The simultaneous refinement of X-ray and neutron diffraction data later confirmed the cationic disorder. Li/Mn substitution thus appears to be an original characteristic which differentiates the present materials from those previously studied.[1–4,6] It has not been possible to prove whether other high-temperature-prepared materials present the same feature. Structural calculations carried out on Hoppe single-crystal data[6] proved inconclusive.

Modelling of the Abnormal Reflection Line (110)

The superposition of two lines could explain the anomalously wide peak situated at $2\theta = 24.8°$. For instance, one of the lines could be that of the $LiMnO_2$ samples themselves, the other possibly being attributable to a badly crystallized impurity. The line has thus been modelled by two peaks using the program PROFILE[11] for the material MN384. The profile parameters obtained during the XRD data refinement (with the zone around $2\theta \approx 24.8°$ indeed excluded) allowed the theoretical profile of the (110) peak to be modelled. From the difference $peak_{obs} - peak_{calc}$, a second peak was obtained (Fig. 8), which could correspond to an interatomic distance of 3.58 Å, attributable to an Mn–Mn distance in the compound Mn_2O_3, one of the precursors of the synthesis of the $LiMnO_2$ samples. The high-temperature phase $LiMnO_2$ synthesized by Davidson *et al.*[4] also exhibits the same anomalously wide peak. This kind of preparation does not use Mn_2O_3 as a precursor, but it may be present as an intermediary phase during the reduction of the manganese dioxide.

Table 6 Values of the deviance criteria obtained for the ordered (Q) and disordered (Q') structure arrangements of the $LiMnO_2$ phases (see text for a definition of Q)

sample	Q	Q'	$(1-Q'/Q)$ (%)
A-type samples			
MN389	18000	14200	21
MN384	6100	4840	20
MN386	12300	8050	35
B-type samples			
MN399	14200	11600	18
MN412	6950	6430	7
MN401	12500	11600	7

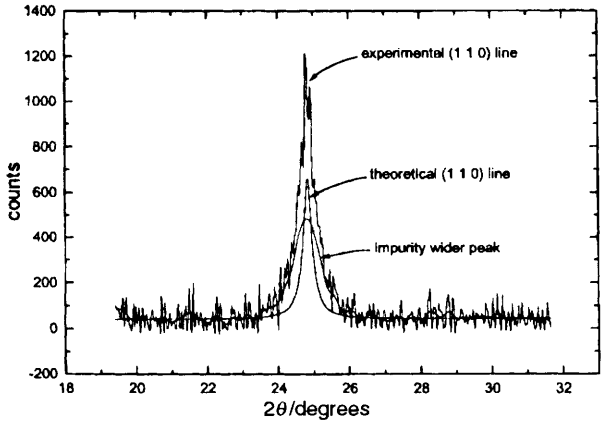

Fig. 8 Decomposition of the $2\theta \approx 24.8°$ X-ray diffraction line of the MN384 sample showing that the peak can result in the combination of the phase (110) line and of an impurity wider peak (poorly crystallized phase)

The theoretical density of stoichiometric $LiMnO_2$ is 4.213. All the A-type compounds show similar densities within three ESDs, but slightly higher than 4.213. As Li_2CO_3 has been detected in these compounds, one should expect a lower density than the stoichiometrically expected value. Since the phases are, within error, necessarily stoichiometric (see synthesis and structure refinement sections) the only way to explain this discrepancy is to take into account another impurity having a higher density than $LiMnO_2$. This material should be Mn_2O_3: it explains the broad line observed in the XRD diagrams and it does not introduce another oxidation state for manganese (only an oxidation state of III is found for Mn in all the syntheses). For the B-type materials, the density decreases on going from MN399 to MN401, in accordance with the increase in Li_2CO_3 content and the quasi-absence of Mn_2O_3, as observed by XRD. This means that some excess of LiOH is necessary to consume Mn_2O_3 fully; this excess probably plays the role of a melt, favouring crystal growth and explaining the occurrence of the larger single crystals of the B-type samples and their better defined XRD patterns (see above).

Conclusion

Through various and accurate measurements, it has been possible to demonstrate that the $LiMnO_2$ samples prepared at high temperature and under reducing atmospheres do show the same *Pmnm* space group as previously reported for the $LiMnO_2$ compounds. However, whereas these latter materials have been described as ordered compounds, the $LiMnO_2$ samples prepared according to ref. 5 exhibit a significant degree of Li/Mn substitution (between 3 and 12%). The disorder introduced to improve the modelling of the powder XRD data is in line with the behaviour of lithium, the size of which allows such a substitution as often observed in oxides. Clearly, the presence of manganese within the lithium sheets may improve the electrochemical behaviour of the disordered materials compared with that of the ordered phases. On the other hand, it is also possible that too high a substitution rate may hamper the lithium diffusion throughout the structure[17] and modify the phase-transition mechanism expected upon lithium deintercalation of $LiMnO_2$. Electrochemical studies are at present under way to attempt to link the electrochemical activity (capacity, energy and reversibility) to the stoichiometry, substitution ratio and morphology of this new $LiMnO_2$ material.

Thanks are due to Alcatel Alsthom Research for financial support.

References

1 T. Ohzuku, A. Ueda and T. Hirai, *Chem. Express*, 1992, **7**, 193.
2 J. N. Reimers, E. W. Fuller, E. Rossen and J. R. Dahn, *J. Electrochem. Soc.*, 1993, **140**, 3396.
3 R. J. Gummow, D. C. Liles and M. M. Thackerary, *Mater. Res. Bull.*, 1993, **28**, 1249.
4 I. J. Davidson, R. S. McMillan, J. J. Murray and J. E. Greedan, *J. Power Sources*, 1995, **54**, 232.
5 A. Lecerf, P. Biensan and S. Baudry, *Fr. Pat. Brevet FR*, 9308484.
6 R. Hoppe, G. Brachtel and M. Jansen, *Z. Anorg. Allg. Chem.*, 1975, **417**, 1.
7 R. D. Shannon, *Acta Crystallogr., Sect. A*, 1976, **32**, 751.

8 J. Rodriguez-Carjaval, *Fullprof manual, ILL Report*, 1992.
9 B. E. Warren, in *Progress in Metal Physics*, ed. Pergamon Press, London, 1959, vol. 8, p. 521.
10 WIN-CRYSIZE Crystallite Size and Microstrain, Siemens, 1991.
11 Diffrac-AT, V3-2, Siemens, 1993.
12 J. B. Goodenough, M. M. Thackeray, W. I. F. David and P. G. Bruce, *Rev. Chim. Miner.*, 1984, **21**, 435.
13 W. I. F. David, M. M. Thackeray, L. A. De Picciotto and J. B. Goodenough, *J. Solid State Chem.*, 1987, **67**, 316.
14 W. I. F. David, M. M. Thackeray, P. G. Bruce and J. B. Goodenough, *Mater. Res. Bull.*, 1984, **19**, 99.
15 W. I. F. David, J. B. Goodenough, M. M. Thackeray and M. G. S. R. Thomas, *Rev. Chim. Miner.*, 1983, **20**, 636.
16 P. Strobel and B. Lambert-Andron, *J. Solid State Chem.*, 1988, **75**, 90.
17 C. D. W. Jones, E. Rossen and J. R. Dahn, *Solid State Ionics*, 1994, **68**, 65.

Paper 5/02130H; *Received* 3*rd April*, 1995